ISBN: 978-3-95450-229-5 ISSN: 2673-5520 doi:10.18429/JACoW-MEDSI2020-WEPA08

INVESTIGATING OF EBW PROCESS WELDMENT CONNECTIONS STRESSES IN ILSF 100 MHz CAVITY BY Simufact.Welding SOFTWARE*

V. Moradi†, Department of Mechanical Engineering, ILSF, Tehran, Iran
A. Adamian, N. B. Arab, Dept. of Mechanical Engineering, Tehran Central Azad Univ., Tehran, Iran

Abstract

The cavity is one of the main components of all accelerators, which is used to increase the energy level of charged particles (electrons, protons, etc.). The cavities increase the energy level of the charged particle by providing a suitable electric field to accelerate the charged particle. Here, information about electron beam welding analysis in 100 MHz cavities of ILSF design will be explained. According to studies performed in most accelerators in the world, connections in cavities are made by various methods such as explosive welding, brazing, electron beam welding, etc. Many articles on large cavities state that the connection of the side doors must be done by the electron beam welding process. However, in the present paper, the three-dimensional model of the cavity is imported into Simufact.Welding software after simplification and mesh process was done, then the heat source of electron beam welding and other welding factors such as beam power, Gaussian distribution, etc. are applied in the software. The purpose of this study is the number of residual stresses during the EBW process in the 100 MHz cavity of ILSF.

INTRODUCTION

Since the early 1970s, finite element modelling has been used to simulate mechanical problems in welding. Some popular sources up to the 1990s are the works of Ueda and Yamakawa [1], Goldak [2] and Radaj [3]. Finite element codes have been described to address these issues among numerous articles such as Dexter [4] and Karlsson [5]. In most finite element models, it is common to assume a number of simplifications. The reason for this simplification is the high computational cost of 3D models (which, of course, is not always approved). However, Duranton et al. [6] showed that when the heat flux in the welding direction is ignored, shortcomings in the two-dimensional method in longitudinal welding will occur.

According to the mechanical explanations of the problem, in some articles such as Song et al. [7] and several other articles, it is assumed that the material acts as a viscous elastoplasty pattern, and in others such as Branza et al. [8], Duranton et al. [6] The assumption of hard isotropic materials, or in other articles such as Nandan et al. [9], has considered the material as an elasto-viscoplastic material. Alberg and Berglund [10] compare the plastic and viscoelastic models used to simulate welding and recommend that a simple plastic model be used in the early stages of the study. However, the viscosity effects of materials at high temperatures cannot be ignored, as they have a significant effect on the behaviour of metals. Also, welding generally involves cooling cycles whose effect on the mechanical behaviour of the material will only be considered if the material is in a state of kinematic hardening. Therefore, the justification for using simpler models such as plastic elastic, without considering the hardening of the material or just the isotropic hardening (which has been the most widely used to date) is only to reduce computational costs. In this paper, the analysis of welding joint calculations in ILSF 100 MHz cavity will be investigated. According to studies performed in most accelerators in the world, the welding connections of the cavities have been done by electron beam. Therefore, in the forthcoming research, the three-dimensional cavity model after simplification and meshing was entered into Simufact.Welding software and then the heat source of electron beam welding and other welding factors such as beam power, Gaussian distribution amount, and etc. Finally, in the software, the simulation of the beam welding process will be done. The purpose of this study is to determine the number of residual stresses in the cavity after the EBW process.

NUMERICAL MODEL OF HEAT SOURCE

The heat source model in the EBW process is combined in such a way that the thermal effect of the key hole in the penetration depth is modelled with a three-dimensional conical heat source and also the molten metal vapor at the weld surface which has its own local thermodynamic equations of the surface heat source. Used by a Gaussian heat source model to simulate the effect of surface heat.

The formula for the distribution of Gaussian heat source is as follows [11]:

$$q_s(x,y) = \frac{3Q_s}{\pi R^2} \times exp\left|-\frac{3(x^2+y^2)}{R^2}\right| \quad (1)$$

Where, (q_s) is the heat flux in the Cartesian coordinates, (Q_s) is the Gaussian heat source power, and (R) is the effective radius of the electron beam. Of course, assuming that (r) is the distance of each point from the heat source to its center, the relation $x^2 + y^2 = r^2$ holds. Also, by moving the welding heat source, the inlet heat flux changes in different positions along the direction of the welding speed. The relationship between moving coordinates and static coordinates is defined as follows:

$$u = y + v(\tau - t) \quad (2)$$

Where, (t) is the welding time, (v) the welding speed and (τ) the time delay factor. After converting the static coordinates to motion coordinates in Eq. (1) we will have:

$$q_s(x,y) = \frac{3Q_s}{\pi R^2} \times exp\left|-\frac{3(x^2+y+v(\tau-t)^2)}{R^2}\right| \quad (3)$$

* Work supported by Iranian Light Source Facility (ILSF)
† v.moradi1985@gmail.com

ISBN: 978-3-95450-229-5 ISSN: 2673-5520 doi:10.18429/JACoW-MEDSI2020-WEPA08

Where, the relation $x^2 + u^2 = r^2$ is assumed. And the distribution of heat flux from the conical heat source in the kinetic coordinates is as follows:

$$q_v(x,y,z) = \frac{9Q_v}{\pi h r_0^2} \times exp\left|-\frac{h^2}{(h-z)^2} \cdot \frac{3(x^2+y+v(\tau-t)^2)}{r_0^2}\right| \quad (4)$$

Where, $q_v(x,y,z)$ is the heat flux within the welding heat source range effective in Cartesian coordinates. (Q_v)The power of the conical heat source and (h) the depth of the electron beam heat source is effective and (z) vary from "0" to "h". The total power of the two welding heat sources $(q_s)$and (q_v) is equal to the effective input power during the welding process, i.e.:

$$Q_s + Q_v = Q \quad (5)$$

Where, (Q) is the effective input power which can be expressed as:

$$Q = CU_aI_b \quad (6)$$

Where, (C) is the effective power factor for the electron beam heat source, (U_a) is the accelerator voltage and (I_b) is the beam current.

If the energy distribution coefficient of the Gaussian surface source is the effective input power (γ_s) and the ratio of the power distribution of the conical heat source to the effective input power (γ_v) and the relation $\gamma_s + \gamma_v = 1$ is established, then we have:

$$Q_s = \gamma_s Q \quad (7)$$

$$Q_v = \gamma_v Q \quad (8)$$

RESULTS

There is the ability to create tracking points in the Simufact.Welding software. Figure 1 (left) shows these points in two paths, 1 and 2, both on the side door. Path 1 passes where the welding line have overlap, but Path 2 is not.

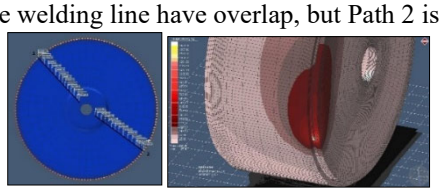

Figure 1: Trace points created on the side door of the cavity (left) Perform the electron beam welding process of the cavity (right).

A view of the cavity electron beam welding process is shown in Fig. 1 (right). In this figure, it is possible to see the key hole effect that exists in the heat source sequence. Figure 2 (left) shows the heat distribution in the parts per 604 seconds of the welding process. According to it, it can be seen that during welding, the areas close to the welding site are heated to about 650 degrees and a little further away to about 400 degrees Celsius. But other parts of the body and side door will be between 100 and 200 degrees Celsius. Figure 2 (right) shows well the HAZ area in this welding process. Due to the expected high penetration depth (18 mm) as well as the high percentage of volumetric heat fraction, the thickness of the HAZ area seems a little bit high.

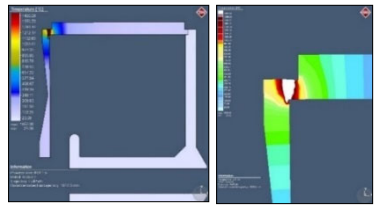

Figure 2: Thermal distribution in parts (left) of heat affected zone (HAZ) in copper cavity analysis (right).

Figure 3 (left) shows the total displacement value at the tracking all points of Route 2. The largest amount of displacement occurred at point 36, as shown in the figure (right), which is about 3.2 mm. This is due to the thinning on the side door to perform the cavity tuning process.

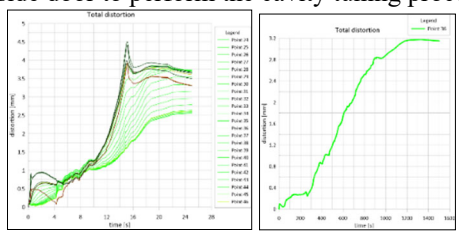

Figure 3: Total deformation value at tracking all points of Route 2 (left) Total deformation value at tracking point 36 from track 2 (right).

In Fig. 4 (left) it can be seen that in 418th seconds of calculations, the heat source passes through the outer edge (point 25) and at this time the stress at the outer edge is zero. Before the heat source reaches this point, the stress is positive (compressive) and then negative (tensile). The outer edge will experience the most negative stress at 473th seconds (55 seconds after the heat source passes through this point), which is about 42 MPa. The stress will then move in the positive direction until the maximum amount of stress is generated at this point, which is equal to about 18 MPa at this point. After that, the tension will decrease but will remain positive. Therefore, the maximum amount of stress remaining at the outer edge at the point where the heat source has passed once will be about 10 MPa. According to Fig. 4, in path 2 and at points that are far from the path of the heat source, about 20 MPa of negative stress will remain.

On other hand, we can compare the outer edges of path 1 and path 2. In Fig. 4 (right) difference between the stress of the outer edge of path 1 (point 04) and the outer edge of path 2 (point 27) is shown, and the point is the amount of residual stress of two edges are too close together.

Figure 4: Stress changes in the tracking points of the outer edge (25) and inner edge (46) of the side door of the cavity in path 2 (left) Stress changes in the tracking points of outer edges of path 1 and path 2 (right).

ISBN: 978-3-95450-229-5 ISSN: 2673-5520 doi:10.18429/JACoW-MEDSI2020-WEPA08

But the most critical point in terms of residual stresses in route 2 is the thinning point on the side door. In Fig. 5 (right) the amount of residual stress at this point can be found, which is equal to 27 MPa. Also, the amount of deformation of this point in the Y direction (the direction of movement of the beam through the cavity) will be equal to -2.3 mm. According to Fig. 5 (left) and comparing the tracking points of Route 1 (where the heat source has twice affected the outer edge areas of this route) with Route 2, it can be seen that the most critical point in terms of residual stress in the whole outer edge of the door The side is on path 1. However, the greatest amount of total deformation in path 1 also belongs to the thinning part of the side door and its value will be equal to 3.7 mm, the share of this value in the Y direction is about -2.8 mm.

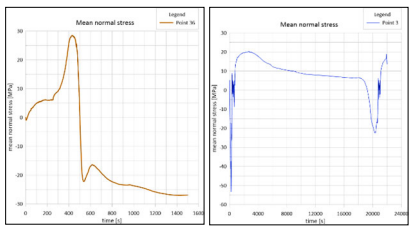

Figure 5: Stress changes in the tracking at point 36 - Side door thinning part - from path 2 (right) The maximum amount of stress remaining in path 1 (left).

VALIDATION OF CALCULATION

In order to improve the production process of a product, some reputable companies in the world raise the existing problems in the form of student and research projects, either within the company itself or in prestigious universities around the world. An example of this is an article by Michael Chiumenti et al. [12] at the Polytechnic University of Catalonia for Airbus.

In this paper, entitled “Numerical analysis of electron beam welding and its practical validation” presented in the journal Finite Elements in Analysis and Design in 2016, a simple model is considered to numerical calculations and practical validation. The numerical calculations were done by COMET code. The dimensions of this model are 290 × 52 × 10.5 mm. To ensure the calculation, this model has been tested in two situations. The difference between the first case and the second case is the location of the thermal sensors during the welding process, as well as the location of the parts by the clamp. Figure 6 shows the studied states. The material intended for calculations is titanium alloy Ti6Al4V.

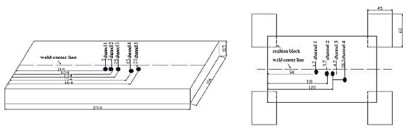

a) Benchmark 1 a) Benchmark 2

Figure 6: Location of thermocouples in position 1 and 2.

Table 1 shows the parameters of the EBW process for welding sample parts. This process is very expensive, so to reduce costs, the EBW of these samples has been done in China “BAMTRI” research laboratory.

Table 1: Electron Beam Welding Parameters of Both Case

Voltage 150 [kV]
Current Intensity 100 [mA]
Speed 25 [mm/s]
Spot Size 1 [mm]
Penetration 10 [mm]

Figure 7 shows a comparison of temperature changes at four similar points from Benchmark 2 analysis in Simufact.welding and COMET software. As can be seen, the consistency of the performed analyses can be seen well. On the other hand, by comparing the HAZ region in the two analyses in Fig. 8, we will find that the calculations performed for welding 100 MHz ILSF cavity with Simufact.Welding software are reliable.

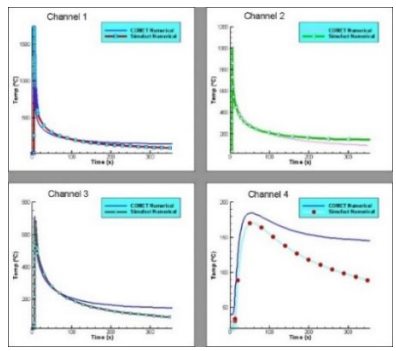

Figure 7: Comparison of temperature changes at four different points of the Benchmark 2 model. Comparison of numerical computing temperatures with COMET software and Simufact.Welding software.

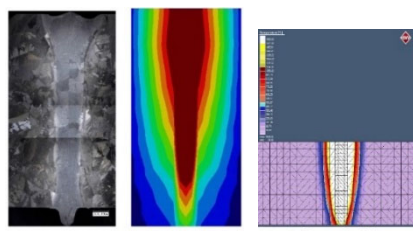

a) Experimental b) Numerical c) Numerical 2

Figure 8: Comparison of HAZ region in empirical evidence (a) and numerical analysis in COMET (b) and numerical analysis in Simufact.welding (c).

CONCLUSION

According to the obtained results and validation, it can be concluded that the boundary conditions defined in the software are correct and appropriate. The amount of heat generated in the weld seam is slightly high, so we can increase the speed of the heat source or reduce the inlet power. In the analysis, the amount of residual stress in the parts is not so high, therefore, there is not a serious need for stress release operation after the EBW process in the 100 MHz ILSF cavity. The amount of deformation in the side doors and especially in the thinning part in this analysis is very high and the side door must be machined to the thin part of it, after the welding process. It is suggested that different methods of mounting to improve the amount of deformation is considered in the next analysis in the future.

ISBN: 978-3-95450-229-5 ISSN: 2673-5520 doi:10.18429/JACoW-MEDSI2020-WEPA08

REFERENCES

[1] Y. Ueda and T. Yamakawa, "Analysis of thermal elastic–plastic stress and strain during welding by finite element method", *Transactions of the Japan Welding Society Transactions*, vol. 2, pp. 186-196, 1971.

[2] J Goldak *et al.*, "Coupling Heat Transfer, Microstructure Evolution and Thermal Stress Analysis in Weld Mechanics", in *Mechanical Effects of Welding*, L Karlsson, L-E Lindgren, M, Jonsson, Eds., Berlin, Heidelberg: Springer, 1992, pp. 1-30.

[3] R. Radaj, "Finite element analysis of welding residual stresses", in *2nd International Conference on Residual Stresses*, *Springer,* Dordrecht, 1989, pp. 510–516. doi:10.1007/978-94-009-1143-7_85

[4] R. Dexter *et al.*, "Residual Stress Analysis in Reactor Pressure Vessel Attachments – Review of Available Software", Southwest Research Institute, San Antonio, TX, Rep. NP-7469, Sep.1991.

[5] L. Karlsson, "Modeling in Welding, Hot Powder Forming, and Casting", ASM International, Ohio, Rep. 0871706164, Dec. 1997.

[6] P. Duranton *et al.*, "3D modeling of multipass welding of a 316L stainless steel pipe", *Journal of Materials Processing,* vol. 153-154, pp. 457–463, Nov. 2004. doi:10.1016/j.jmatprotec.2004.04.128

[7] J. Song *et al.*, "Sensitivity analysis of the thermomechanical response of welded joints", *Int. J. Solids Struct.,* vol. 40, pp. 4167–4180, Aug. 2003. https://doi.org/10.1016/S0020-7683(03)00223-3

[8] T. Branza *et al.*, "Experimental and numerical investigation of the weld repair of superplastic forming dies", *J. Mater. Process. Technol.,* vol. 155–156, p. 1673–1680, Nov. 2004. doi:10.1016/j.jmatprotec.2004.04.388

[9] R. Nandan *et al.*, "Numerical modelling of 3D plastic flow and heat transfer during friction stir welding of stainless steel", *Sci. Technol. Weld. Joining*, vol. 11, p. 526–537, Dec. 2006. doi:10.1179/174329306X107692

[10] H. Alberg and D. Berglund, "Comparison of plastic, viscoplastic, and creep models when modelling welding and stress relief heat treatmen", *Comput. Methods Appl. Mech. Eng*, vol. 192 , pp. 5189–5208, Sep. 2003. doi:10.1016/J.CMA.2003.07.010

[11] Y. Luo *et al.*, "Simulation on welding thermal effect of AZ61 magnesium alloy based on three-dimensional modeling of vacuum electron beam welding heat source", *Vacuum*, vol. 84 p. 890–895, Mar. 2010. doi:10.1016/j.vacuum.2009.12.005

[12] M. Chiumenti *et al.*, "Numerical modeling of the electron beam welding and its experimental validation", *Finite Elem. Anal. Des.,* vol. 121, pp. 118-133, Nov. 2016. doi:10.1016/j.finel.2016.07.003